



Contents lists available at ScienceDirect

Journal of Controlled Release

journal homepage: [www.elsevier.com/locate/jconrel](http://www.elsevier.com/locate/jconrel)

## Revisit complexation between DNA and polyethylenimine – Effect of uncomplexed chains free in the solution mixture on gene transfection

Yanan Yue<sup>a,\*</sup>, Fan Jin<sup>a</sup>, Rui Deng<sup>a</sup>, Jing Cai<sup>a</sup>, Yangchao Chen<sup>b</sup>, Marie C.M. Lin<sup>c</sup>, Hsiang-Fu Kung<sup>b</sup>, Chi Wu<sup>a,d,\*</sup>

<sup>a</sup> Department of Chemistry, The Chinese University of Hong Kong, Shatin, N.T., Hong Kong

<sup>b</sup> Stanley Ho Center for Emerging Infectious Diseases, The Chinese University of Hong Kong, Shatin, N.T., Hong Kong

<sup>c</sup> Institute of Molecular Biology, Department of Chemistry, The University of Hong Kong, Pokfulam Road, Hong Kong

<sup>d</sup> The Hefei National Laboratory of Physical Science at Microscale; Department of Chemical physics, The University of Science and Technology of China, Hefei, Anhui 230026, China

### ARTICLE INFO

#### Article history:

Received 12 June 2010

Accepted 22 October 2010

Available online xxx

#### Keywords:

Gene delivery

DNA condensation

Free polyethylenimine

Laser light scattering

Cellular internalization

### ABSTRACT

Our revisit of the complexation between anionic DNA and cationic polyethylenimine (PEI) in both water and phosphate buffered saline (PBS) by using a combination of laser light scattering (LLS) and gel electrophoresis confirms that nearly all the DNA chains are complexed with PEI to form polyplexes when the molar ratio of nitrogen from PEI to phosphate from DNA (N:P) reaches ~3, but the PEI/DNA polyplexes have a high *in-vitro* gene transfection efficiency only when  $N:P \geq 10$ . Putting these two facts together, we not only conclude that this extra 7 portions of PEI chains are free in the solution mixture, but also confirmed that it is these free PEI chains that substantially promote the gene transfection no matter whether they are applied hours before or after the administration of the much less effective PEI/DNA polyplexes ( $N:P=3$ ). The uptake kinetics measured by flow cytometry shows that the addition of free PEI leads to a faster and more efficient cellular internalization of polyplexes, but these free PEI chains mainly contribute to the subsequent intracellular trafficking. In contrast, the bound PEI chains mainly play a role in the DNA condensation and protection, leading to a different thinking in the development of non-viral vectors.

© 2010 Elsevier B.V. All rights reserved.

### 1. Introduction

In comparison with viral vectors, more efforts have recently been spent on the development of non-viral vectors because of few fatal accidents in clinical trials of viral carriers [1–3]. It has been well recognized that non-viral vectors have their own advantages, such as low immune toxicity, construction flexibility and facile fabrication, in the gene transfection, especially for clinical applications [4–6]. However, they are still much less efficient than their viral counterparts. Among thousands of experimentally tested non-viral vectors, cationic polyethylenimine (PEI) is still considered as one of the most efficient candidates to deliver genes and often served as a “golden standard” [7–9]. Previously, PEI has been chemically modified in different ways so that additional functions were introduced for a better gene delivery, including the incorporation of intracellular biodegradable linkers [10,11], the PEGylation to improve the serum stability during circulation [12,13] and the attachment of some functional molecules to target specific cells or tissues [12–15]. Less attention, however, has been paid to why PEI remains one of the best

non-viral carriers and how it facilitates the intracellular trafficking [16–27].

The first step in the development of non-viral vectors is how to package long anionic DNA chains into a small particle, i.e., the DNA complexation and condensation. Previous study showed that the physical and colloidal characteristics of resultant polymer/DNA polyplexes are important for an effective delivery of gene [28–32], but results were controversial and not conclusive. Much of the past effort has been devoted to the synthesis of state-of-the-art polymers [33–37] and subsequent polyplex formation [38–41], rather than the fundamental understanding of how a non-viral vector promotes the intracellular trafficking of DNA besides its roles in DNA condensation and protection. The proposed proton-sponge effect has been well accepted and taken as granted by those who entered this field later [7,42].

Using a combination of different methods to characterize the size, molar mass and surface charge of the PEI/DNA polyplexes formed under different conditions, we confirmed some of the previous literature results, but revealed that the average size and chain density of the resultant polyplexes are not that important in the gene transfection. In order to achieve an optimal transfection efficiency, the polyplexes in the solution mixture should have a slightly positively charged surface with a N:P ratio higher than 10. It is understandable that a positively charged surface facilitates the

\* Corresponding authors. Department of Chemistry, The Chinese University of Hong Kong, Shatin, N.T., Hong Kong. Tel.: +852 2609 6266; fax: +852 2603 5057.

E-mail addresses: [yananyue.linda@gmail.com](mailto:yananyue.linda@gmail.com) (Y. Yue), [chiwu@cuhk.edu.hk](mailto:chiwu@cuhk.edu.hk) (C.Wu).

attachment of polyplexes to the negatively charged cellular membrane so that the endocytosis is promoted. However, it is still not clear why a high N:P ratio is required. Few previous studies showed that when the N:P ratio is high, a large amount of PEI chains are free in the solution mixture of DNA and PEI [43,44]. It was also revealed that these excessive polycationic chains are much more toxic than those bound to DNA inside the polyplexes [44,45]. Moreover, Wagner and his coworkers found that the removal of free PEI chains by size exclusion chromatography significantly reduced the gene transfection efficiency [44]. To our knowledge, only few previous studies have noted such an effect of free polycationic chains on the gene transfection [43–47]. Most of the researchers in this field have overlooked such a finding. The current study was designed to elucidate the impact of polymer chains free in the solution mixture on gene delivery.

## 2. Materials and methods

### 2.1. Materials and cell lines

Branched PEI with a weight-averaged molar mass of 25,000 g/mol (bPEI-25 K, Sigma-Aldrich) was used without further purification. Initial plasmid DNA pGL3-control vector (5,256 bp) encoding modified firefly luciferase and pEGFP-N1 (4,700 bp) expressing enhanced green fluorescent protein (EGFP) were purchased from Promega (USA) and Clontech (Germany), respectively. A large amount of these plasmids were prepared using a Qiagen Plasmid Maxi Kit (Qiagen, Germany). POPO-3 iodide, fluorescein-5-isothiocyanate (FITC) and di-4-ANEPPDHQ were purchased from Invitrogen (USA). Fetal bovine serum (FBS), Dulbecco's modified Eagle's medium (DMEM) and penicillin-streptomycin were purchased from GIBCO (USA). 293 T cells were grown at 37 °C, 5% CO<sub>2</sub> in DMEM supplemented with 10% FBS, penicillin at 100 units/mL and streptomycin at 100 µg/mL.

### 2.2. Formation of PEI/DNA polyplexes

Plasmid DNA was complexed with PEI in either distilled water or phosphate buffered saline (PBS) to form the PEI/DNA polyplexes as follows. Different amounts of PEI solution ( $C = 1 \times 10^{-4} - 1 \times 10^{-3}$  g/mL) were added dropwise into a dilute DNA solution ( $C = 14.5$  µg/mL), resulting in different molar ratios of nitrogen from PEI to phosphate from DNA (N:P). Each resultant PEI/DNA dispersion was incubated for 5 min at room temperature before its administration to the cell culture medium.

### 2.3. DNA binding assay

The binding of DNA to PEI to form polyplexes in the solution mixture was evaluated by the gel-shift assay. Each PEI/DNA dispersion with a desired N:P ratio was mixed with 6× loading buffer (bromophenol blue/xylene cyanol) and then loaded on a 0.8% (w/v) agarose gel containing ethidium bromide in tris-borate EDTA buffer. The amount of DNA loaded into each well was 0.4 µg in a total volume of 10 µL. The electrophoresis was performed under 100 V for 45 min. DNA bands were visualized under UV. The DNA binding was also characterized using laser light scattering (LLS).

### 2.4. POPO-3 fluorescence quenching assay

Plasmid was labeled with POPO-3 dye at 1 dye to 100 base pair ratio. PEI/DNA polyplexes with different N:P ratios were prepared as described above. The final DNA concentration is 1.45 µg per 100 µL solution. After a 5-min incubation, the relative fluorescence intensity ( $F$ ) of each solution mixture was collected using a Hitachi F4500 fluorescence spectrophotometer (excitation 530 nm, emission

570 nm). The fraction of the uncomplexed DNA chains ( $x$ ) was determined by  $x = (F_{\text{polyplex}} - F_{\text{blank}}) / (F_{\text{DNA}} - F_{\text{blank}})$ .

### 2.5. Laser light scattering

A commercial LLS instrument (ALV5000) with a vertically polarized 22-mV He-Ne laser (632.8 nm, Uniphase) was used. The measurable angular range is 15–154°. In dynamic LLS, the intensity–intensity time correlation function ( $G^{(2)}(\tau)$ ) of each PEI/DNA polyplex solution mixture was measured at different scattering angles. The Laplace inversion of each  $G^{(2)}(\tau)$  can lead to a line-width distribution of  $G(\Gamma)$  by the CONTIN program or by the double-exponential fitting, if there are only two relaxation modes, as

$$\left\{ \left[ G^{(2)}(q, \tau) - B \right] / B \right\}^{1/2} = A_1(q) e^{-\langle \Gamma \rangle_1 \tau} + A_2(q) e^{-\langle \Gamma \rangle_2 \tau} \quad (1)$$

where  $B$  is the measured baseline;  $\langle \Gamma \rangle$  and  $A(q)$  are the average line-width and the normalized intensity contribution of each relaxation mode, respectively, and  $A_1(q) + A_2(q) \equiv 1$ ;  $q$  is the scattering vector defined as  $q \equiv (4\pi n / \lambda_0) \sin(\theta/2)$  with  $\theta$ ,  $\lambda_0$  and  $n$ , the scattering angle, the incident wavelength in vacuum and the refractive index of solvent, respectively.  $\langle \Gamma \rangle$  can be related to the average translational diffusion coefficient  $\langle D \rangle$  as  $\langle \Gamma \rangle = \langle D \rangle q^2$ . Using the Stokes–Einstein equation [48],  $\langle D \rangle$  is further related to the average hydrodynamic radius ( $\langle R_h \rangle$ ) by  $\langle R_h \rangle = k_B T / (6\pi \eta \langle D \rangle)$ , where  $\eta$  is the solvent viscosity. In this way, each  $G(\Gamma)$  can also be converted into a hydrodynamic radius distribution  $f(R_h)$ .

On the other hand, the time-averaged scattering intensity from each relaxation mode can be calculated from the total time-averaged scattering intensity ( $\langle I(q) \rangle$ ) and  $A(q)$ , respectively, measured from static and dynamic LLS, i.e.,  $\langle I(q) \rangle_1 = \langle I(q) \rangle A_1(q)$  and  $\langle I(q) \rangle_2 = \langle I(q) \rangle A_2(q)$ . The plot of  $1/\langle I(q) \rangle_1$  or  $1/\langle I(q) \rangle_2$  versus  $q^2$  leads to an average radius of gyration ( $\langle R_g \rangle_1$  or  $\langle R_g \rangle_2$ ) and the time-averaged scattering intensity at  $q \rightarrow 0$  ( $\langle I(0) \rangle_1$  or  $\langle I(0) \rangle_2$ ) using [48,49]

$$\frac{1}{\langle I(q) \rangle} \approx \frac{1}{\langle I(0) \rangle} \left( 1 + \frac{1}{3} \langle R_g^2 \rangle q^2 \right) \quad (2)$$

where  $\langle I(0) \rangle$  is proportional to the weight-averaged molar mass. Therefore, individual short PEI chains with a much lower molar mass are invisible in LLS when long DNA chains exist in the solution mixture. The formation of PEI/DNA polyplexes with some DNA chains collapsed inside leads to a relaxation mode faster than that of individual swollen DNA chains. This is why we mainly focused on how N:P ratio affects the fast mode in the current study.

### 2.6. Zeta-potential measurement

The average mobility ( $\mu_E$ ) of the polyplexes under an electric field in an aqueous solution was determined from the frequency shift in a laser Doppler spectrum using a commercial zeta-potential spectrometer (ZetaPlus, Brookhaven) with two platinum-coated electrodes and one He-Ne laser as the light source. Each data point in the mobility measurement was averaged over 20 times at 20 °C. The zeta-potential ( $\zeta_{\text{potential}}$ ) can be calculated from  $\mu_E$  using  $\mu_E = 2\varepsilon \zeta_{\text{potential}} f(\kappa R_b) / (3\eta)$ , where  $\varepsilon$  is the permittivity of water and  $1/\kappa$  is the Debye screening length [50]. When  $\kappa R_b \ll 1$  (the Hückel limit),  $f(\kappa R_b) \approx 1$ ; while  $\kappa R_b \gg 1$  (the Smoluchowski limit),  $f(\kappa R_b) \approx 1.5$ . In the current study, the Hückel and Smoluchowski limits are respectively used to calculate  $\zeta_{\text{potential}}$  in water and PBS.

### 2.7. Determination of the content of free PEI in PEI/DNA dispersion

The content of free PEI in the PEI/DNA dispersion was determined using a combination of filtration and copper complex assay. The PEI/DNA

dispersion at N:P = 10 was prepared as described above, with a final concentration of 219  $\mu\text{g}$  pGL3 per 1 mL PBS. After a 4-h incubation, the PEI/DNA dispersion was centrifuged and the supernatant was carefully filtered using a 20-nm filter. The content of uncomplexed PEI chains in the filtrate was determined using a copper complex assay by adding 100  $\mu\text{L}$  of the filtrate into 900  $\mu\text{L}$  of 0.02 M cupric acetate solution containing 5% potassium acetate (pH 5.5). The absorption of the filtrate was recorded at 630 nm ( $A_{630}$ ) using a UV–vis spectrometer (Hitachi, Japan), and converted to the corresponding PEI concentration according to the calibration curve.

### 2.8. *In vitro* gene transfection

The *in vitro* gene transfection efficiency was quantified by using the luciferase transfection assays, in which plasmid pGL3 was used as an exogenous reporter gene. 293 T cells were plated in a 48-well plate at an initial density of  $1.5 \times 10^5$  per well, 24 h prior to transfection. The PEI/DNA dispersion with a desired N:P ratio was further diluted in serum-free medium and then added at a final concentration of 0.4  $\mu\text{g}$  DNA per well. The complete DMEM medium (800  $\mu\text{L}$  per well) was added 6 h after the gene transfection. Using a GloMax 96 microplate luminometer (Promega, USA) and the Bio-Rad protein assay reagent, we respectively determined the transgene expression level and corresponding protein concentration in each well 48 h after the polyplex administration. The gene transfection efficiency is expressed as a relative luminescence unit (RLU) per cellular protein (mean  $\pm$  SD of triplicates). Alternatively, the transfection efficiency can be directly visualized under a fluorescence microscopy when the plasmid pEGFP-N1 is used.

### 2.9. Cytotoxicity assay

The cytotoxicity of free PEI chains and PEI/DNA dispersion was evaluated on 293 T cells by using the MTT assay. 293 T cells were seeded in a 96-well plate at an initial density of 5000 cells/well. After 24 h, free PEI chains alone or with DNA to form PEI/DNA dispersion were respectively added to cells at different chosen concentrations and N:P ratios. For the PEI/DNA dispersion, the final DNA concentration is 0.2  $\mu\text{g}$ /well in a total volume of 100  $\mu\text{L}$ . The treated cells were incubated in a humidified environment with 5%  $\text{CO}_2$  at 37  $^\circ\text{C}$  for 48 h. The MTT reagent (in 20  $\mu\text{L}$  PBS, 5 mg/mL) was then added to each well. The cells were further incubated for 4 h at 37  $^\circ\text{C}$ . The medium in each well was then removed and replaced by 100  $\mu\text{L}$  DMSO. The plate was gently agitated for 15 min before the absorbance ( $A$ ) at 490 nm was recorded by a microplate reader (Bio-rad, USA). The cell viability ( $y$ ) was calculated by  $y = (A_{\text{treated}}/A_{\text{control}}) \times 100\%$ , where  $A_{\text{treated}}$  and  $A_{\text{control}}$  are the absorbance of the cells cultured with polymer/polyplex and fresh culture medium, respectively. Each experiment condition was done in quadruple. The data was shown as the mean value plus a standard deviation ( $\pm$  SD).

### 2.10. DNA, PEI labeling and flow cytometry

Plasmid pGL3 was covalently labeled with the fluorophore Cy5 using the Label IT kit (Mirus, Madison, WI) according to the manufacturer's instructions. For labeling of PEI, 11.2 mg of FITC (28.8  $\mu\text{mol}$ ) was mixed with 360 mg of bPEI-25 K (14.4  $\mu\text{mol}$ ) in EtOH, and the reaction mixture was stirred overnight at room temperature in the dark place. In order to separate labeled PEI from unreacted FITC, size exclusion chromatography (SEC) was performed using a gel-filtration column (Sephadex G-25 superfine) preequilibrated with HBS (20 mM HEPES, pH 7.4, 150 mM NaCl). The separated sample was freeze-dried and resolved in water. The gel electrophoresis results confirmed that the labeling on DNA and PEI chains has no obvious impact on the formation of PEI/DNA polyplexes (data not shown).

To explore the effect of free PEI chains on the cellular uptake of polyplexes, FITC-PEI, PEI/Cy5-pGL3 polyplexes alone (N:P = 3) or polyplexes plus 7 portions of free FITC-PEI (N:P = 10) were added to the cells in serum-free DMEM and, after incubation at 37  $^\circ\text{C}$ , cells were harvested at the indicated time points. Briefly, cells were first rinsed twice with PBS containing 0.001% SDS and then PBS to remove the extracellularly attached polyplexes [51]. Further, cells were detached by 0.05% trypsin/EDTA supplemented with 20 mM sodium azide to prevent further endocytosis [52]. Finally, cells were washed twice by pelleting and then resuspended in ice-cold PBS containing 2% FBS. To ensure the effective removal of polyplexes from the cell surfaces, confocal microscopy images of cells were taken and shown in Fig. S1. Cellular uptake of polyplexes and free PEI chains was assayed by flow cytometry using a FC 500 flow cytometry system (Beckman Coulter, USA). The fluorophores FITC and Cy5 were excited at 488 and 635 nm, respectively, and the corresponding emissions were detected at 525/10 and 675/15 nm, respectively. To discriminate viable cells from dead cells and to exclude doublets, the cells were appropriately gated by forward/side scattering and pulse width.  $1 \times 10^4$  gated events per sample were collected. Experiments were performed at least in triplicates.

### 2.11. Confocal laser scanning microscopy

$6 \times 10^5$  cells were seeded in a  $\mu\text{-Dish}^{35\text{mm, high}}$  (ibidi GmbH, Germany). After 24 h, the cellular membrane was stained with di-4-ANEPPDHQ for 15 min and then washed 2–3 times. Afterwards, the cell culture medium was carefully aspirated and FITC-labeled bPEI-25 K in serum-free DMEM was applied at a final concentration of  $1 \times 10^{-5}$  g/mL. Live cell imaging was performed for 1.5 h using a Nikon C1si confocal laser scanning microscope equipped with a spectral imaging detector (Nikon, Japan) and a INU stage-top incubator (Tokai Hit, Japan). Image sequences were captured at approximately 30 s intervals. FITC and di-4-ANEPPDHQ were visualized by the 488-nm excitation and the corresponding emission spectral was acquired in the 495–650 nm range at 5-nm wavelength resolution. The mean FITC-PEI fluorescence intensities at the cellular membrane and inside the cell are recorded at 520 nm and normalized by that outside the cell. All the spectral data was analyzed using the Nikon EZ-C1 software.

## 3. Results and discussion

To investigate the complexation profiles of PEI-mediated vectors, we first monitored the formation of PEI/DNA polyplexes in phosphate buffered saline (PBS) using a combination of static and dynamic laser light scattering (LLS). Fig. 1 shows the N:P ratio dependence of hydrodynamic radius distribution ( $f(R_h)$ ) of pGL3 without and with the addition of different amounts of PEI. In the pure pGL3 solution (N:P = 0.00), the peak located at  $\sim 1.4 \mu\text{m}$  represents the swollen and extended DNA chains. The addition of a small amount of branched PEI (N:P = 0.25) leads to a new peak located at  $\sim 120 \text{ nm}$ , presumably corresponding to the newly formed contracted PEI/DNA polyplexes. The shifting of the DNA peak from  $\sim 1.4 \mu\text{m}$  to  $\sim 1 \mu\text{m}$  indicates the partial contraction of DNA chains due to the incomplete complexation. Further addition of PEI leads to polyplexes of a larger size with more DNA and PEI chains incorporated into the individual complexes. When N:P  $\sim 3$ , the DNA peak completely disappears, suggesting that nearly all the DNA chains are complexed with PEI, i.e., no DNA chains are free in the solution mixture.

The complexation between PEI and DNA was also evaluated by the gel-shift assay (Fig. 2a). Progressive condensation can be revealed from the retarded mobility of the DNA bands and their reduced fluorescence intensity. Clearly, the two DNA bands (supercoiled and relaxed forms) disappear when N:P  $\sim 3$ . Furthermore, we quantitatively estimated the extent of DNA complexation at each given N:P

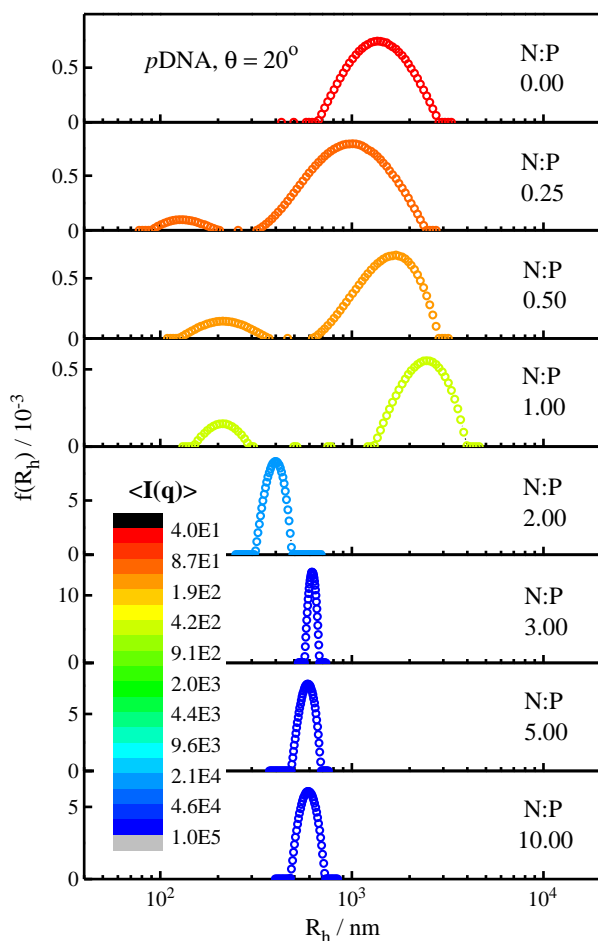


Fig. 1. N:P ratio dependence of the normalized hydrodynamic radius distribution ( $f(R_h)$ ) of PEI/DNA polyplexes formed in PBS, where different colors represent variation of the time-averaged scattering intensity of the solution mixture ( $\langle I(q) \rangle$ ).

ratio using a double-strand DNA intercalating dye, POPO-3, whose fluorescence is dramatically increased upon its binding to DNA. The complexation of DNA with PEI excludes POPO-3 molecules from the DNA double helix, resulting in a reduced fluorescence emission intensity. Fig. 2b shows that over 90% of the DNA chains have been condensed into the polyplexes when  $N:P \sim 3$ . In static LLS, we also found that the average scattering intensity ( $\langle I(0) \rangle$ ) nearly remains a constant after  $N:P \geq 3$ .

It is known that  $\langle I(0) \rangle \sim KCM_w \sim (dn/dc)^2 CM_w$ . Therefore, we can calculate the apparent weight-averaged molar mass ( $M_{w, polyplex}$ ) of the polyplexes at each given N:P ratio using

$$M_{w, polyplex} = M_{w, DNA} \times \frac{\langle I(0) \rangle_{polyplex} C_{DNA} \left(\frac{dn}{dc}\right)_{DNA}^2}{\langle I(0) \rangle_{DNA} C_{polyplex} \left(\frac{dn}{dc}\right)_{polyplex}^2} \quad (3)$$

where  $C$  is concentration and  $(dn/dc)$  is the differential refractive index increment. Note that  $(dn/dc)_{polyplex} = w_{DNA}(dn/dc)_{DNA} + w_{PEI}(dn/dc)_{PEI}$ , where  $w_{DNA}$  and  $w_{PEI}$  are two normalized weight fractions of DNA and PEI inside the polyplexes, i.e.,  $w_{DNA} + w_{PEI} = 1$ . It is necessary to estimate  $C_{polyplex}$  and  $w_{PEI}$  in order to calculate  $M_{w, polyplex}$ . When  $N:P \leq 3$ , we can assume that nearly all the PEI chains are complexed with DNA, while the fraction of DNA associated with PEI can be estimated using the POPO-3 fluorescence assay mentioned above. Therefore,

$$C_{polyplex} = C_{PEI} + (1-x)C_{DNA} \text{ and } w_{PEI} = C_{PEI} / C_{polyplex} \quad (4)$$

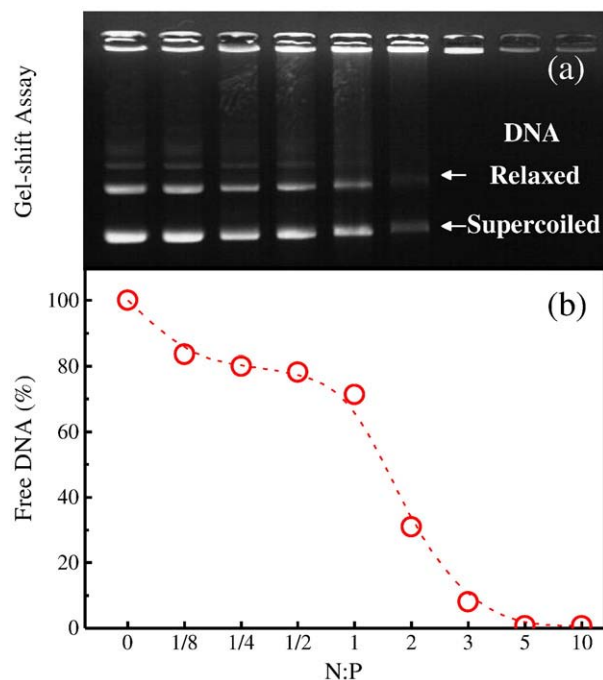
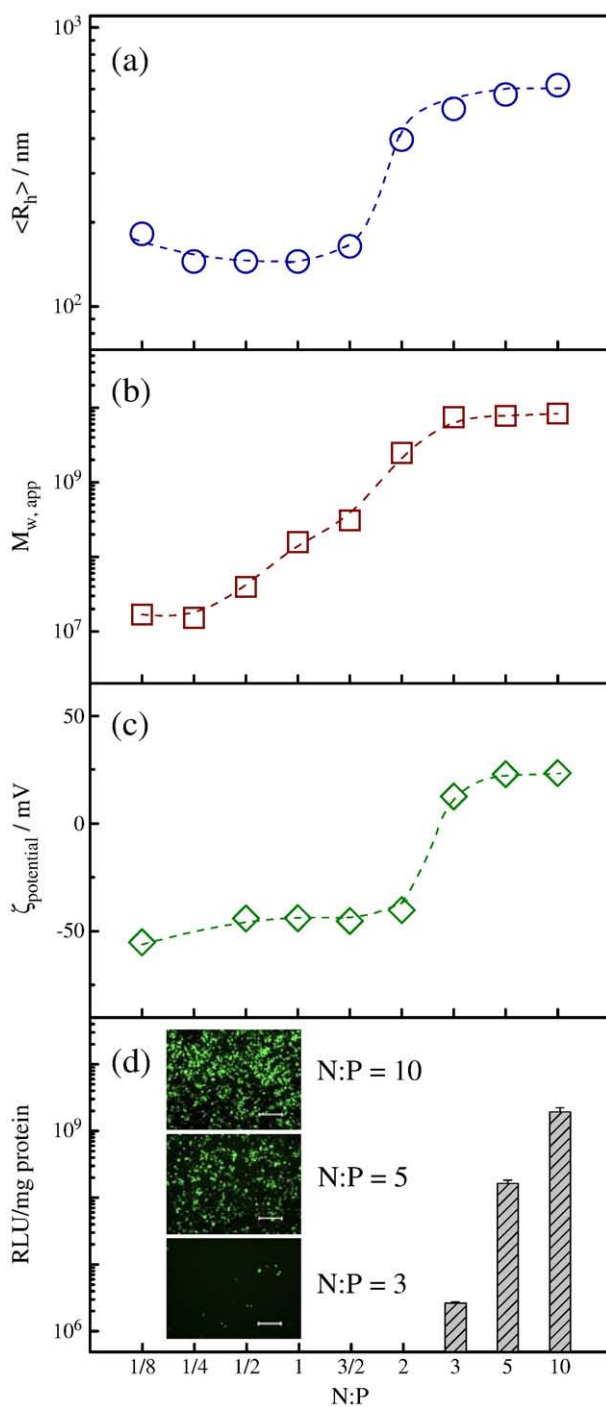


Fig. 2. Complexation profile between PEI and DNA in PBS at different N:P ratios, evaluated by (a) gel-shift assay and (b) POPO-3 fluorescence quenching assay.

where  $C_{PEI}$  and  $C_{DNA}$  are the initial PEI and DNA concentrations, respectively; and  $x$  is the fraction of those uncomplexed DNA chains in the solution mixture. On the other hand, when  $3 < N:P \leq 10$ , nearly all the DNA chains are complexed with PEI so that  $C_{polyplex}$  is a constant in this range and  $C_{polyplex} \approx C_{polyplex} (N:P=3)$ . In the current study,  $C_{DNA} = 1.45 \times 10^{-5}$  g/mL,  $(dn/dc)_{DNA} = 0.362$  mL/g, and  $(dn/dc)_{PEI} = 0.218$  mL/g, measured using a novel laser differential refractometer [53].

Fig. 3 summarizes the N:P ratio dependence of the average hydrodynamic radius ( $\langle R_h \rangle$ ), the apparent weight-averaged molar mass ( $M_{w, polyplex}$ ), the zeta-potential ( $\zeta_{potential}$ ) and the gene transfection efficiency (RLU/mg protein) of the PEI/DNA polyplexes formed in PBS. The initial decrease of  $\langle R_h \rangle$  and increases of both  $M_{w, polyplex}$  and  $\zeta_{potential}$  upon the addition of PEI ( $N:P = 0.125 - 1.50$ ) indicate that the positively charged PEI chains are gradually complexed with the negatively charged DNA chains so that both PEI and DNA contract in the solution mixture. The sharp increases of both  $\langle R_h \rangle$  and  $M_{w, polyplex}$  at  $N:P \sim 2$  reflect the merge of initially formed small polyplexes. Further addition of PEI in the range of  $N:P > 3$  has nearly no effect on  $\langle R_h \rangle$ ,  $M_{w, polyplex}$  and  $\zeta_{potential}$ , clearing revealing that those PEI chains added afterwards are free in the solution mixture.

Only few previous studies have noted the existence of free PEI, and estimated the amount of those free polycationic chains in the PEI/DNA dispersion used for gene delivery. Clamme J.P. et al. found that, by using a two photon fluorescence correlation spectroscopy,  $\sim 86\%$  of the PEI chains are in the free form at  $N:P = 10$  (i.e., polyplexes is completely formed at  $N:P \sim 1.4$ ) [43], whereas Wagner and his coworkers showed that the purified polyplexes by SEC have an ultimate N:P ratio of  $\sim 2.5$  [44]. Our LLS results here clearly shows that the anionic DNA chains are not fully condensed by the cationic PEI chains when  $N:P \sim 1.4$ , also reflected in its corresponding negative zeta-potential of the resultant polyplexes. Besides LLS, herein we used a simple filtration method combined with copper complex assay to determine the content of uncomplexed PEI chains in the PEI/DNA dispersion. Fig. 4 shows that the PEI concentration after the removal of the polyplexes by a 20-nm filter is  $\sim 68.6\%$  of the initial PEI concentration at  $N:P = 10$ , further confirming that DNA is fully condensed by PEI only when  $N:P \geq 3$ . For  $N:P = 10$ ,  $\sim 70\%$  of the PEI



**Fig. 3.** N:P ratio dependence of (a) average hydrodynamic radius ( $\langle R_h \rangle$ ); (b) apparent weight-averaged molar mass ( $M_{w, polyplex}$ ); (c) average zeta-potential ( $\zeta_{potential}$ ); and (d) gene transfection efficiency (RLU/mg protein) of polyplexes formed in PBS. Inset: Fluorescent microscopic images of 293 T cells transfected with pEGFP-N1 after 48 h. Scale bar: 200  $\mu$ m.

chains are free in the solution mixture of PEI and DNA. On the other hand, our results in Fig. 3d consolidate that the polyplexes with 7 portions of free PEI chains (N:P = 10) are  $\sim 10^3$  times more efficient in the gene transfection than those formed at N:P = 3 without free PEI chains.

Previous literature also repeatedly showed that when N:P  $\geq 3$ , nearly all the DNA chains are completely complexed with PEI, but a higher N:P ratio leads to much better gene transfection. Putting these two experimental facts together, one should ask an obvious, but

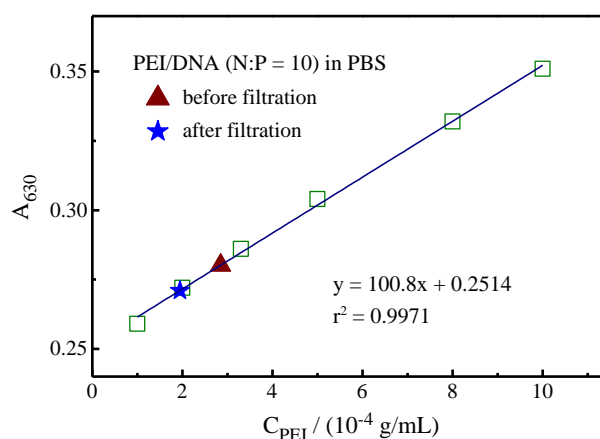


**Fig. 4.** Concentration calibration curve of bPEI-25 K chains in PBS, where symbols  $\blacktriangle$  and  $\star$  refer to the concentration of PEI in PEI/DNA dispersion (N:P = 10) before and after the removal of the polyplexes, respectively.

certainly overlooked, question; namely, is it the free PEI chains, rather than those inside the PEI/DNA polyplexes, that play a vital role in the gene transfection? To generalize such a question, we have tested PEI-mediated vectors with different chain lengths in both salt-free water and salt-rich PBS. All of our results (not shown here) confirm that the solution mixture with polyplexes alone have a much lower gene transfection efficiency.

On the other hand, we evaluated the cytotoxicity of free PEI chains and the corresponding PEI/DNA dispersion on 293 T cells using the MTT assay (Fig. 5). The initial cell viability of PEI/DNA at N:P = 3 is  $\sim 85\%$ , and is stably reduced as the increasing amount of free PEI chains, especially when  $C_{PEI} \geq 2.7 \mu\text{g/mL}$ , corresponding to N:P  $\geq 10$ , clearing revealing that those free PEI chains are indeed the major cause of toxicity of PEI/DNA at high N:P ratios. It is also worth noting that in the general N:P range for transfection, i.e., N:P  $\leq 10$ , both the PEI/DNA dispersion and free PEI chains exhibit relatively low cytotoxicity, with the cell viability well above 70%.

Furthermore, we decided to add the 7 portions of free PEI chains at different times; namely, hours *before* or *after* the administration of the PEI/DNA polyplexes (N:P = 3), so that the final and total N:P ratio remains 10. We define  $t = 0$  for the simultaneous addition of the PEI/DNA polyplexes (N:P = 3) and 7 portions of free PEI chains. Therefore, the negative time means that free PEI chains are added before the polyplex administration. Fig. 6 shows that in the presence of free PEI chains, the transfection efficiency is typically  $10^2$ – $10^3$  times higher than that without free chains no matter whether these free

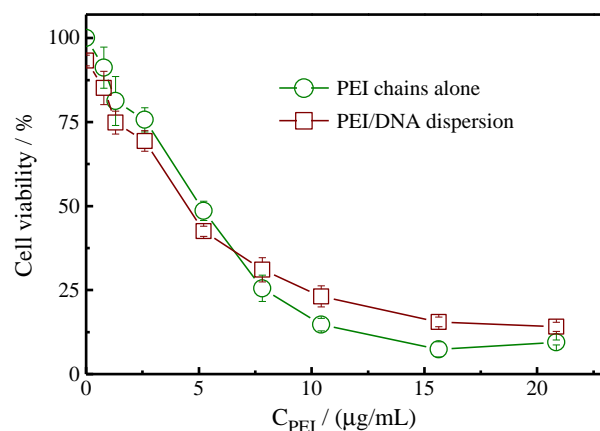


**Fig. 5.** PEI concentration dependence of 293 T cell viability in terms of free PEI chains alone and PEI/DNA dispersions, where  $C_{PEI} = 2.7 \mu\text{g/mL}$  is corresponding to N:P = 10.

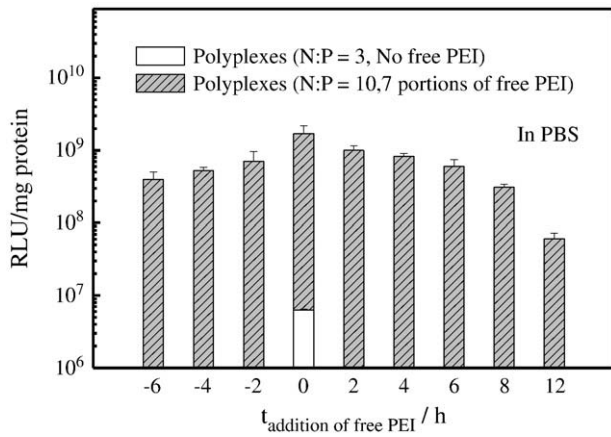


Fig. 6. Effect of 7 portions of free PEI chains added at different times (prior to or post the administration of polyplexes formed at N:P = 3) on the gene transfection efficiency in 293 T cells, where the total and final N:P ratio is kept to be 10 and the cell culture medium is not replaced before the addition of free PEI chains.

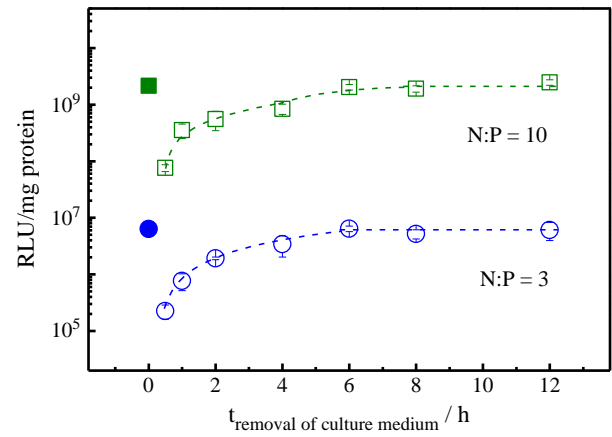


Fig. 8. Effect of removal of cell culture medium on the gene transfection efficiency of PEI/DNA polyplexes formed in PBS with and without free PEI chains in the solution mixture, where “t = 0” means that no cell culture medium was replaced.

polyplexes are introduced before or after the polyplex administration. To our knowledge, this is the first demonstration that the addition of free PEI chains even prior to the polyplexes can facilitate the gene transfection. It is clear that the simultaneous addition of the polyplexes (N:P = 3) and free polycationic chains (i.e., t = 0) leads to the highest transfection level, indicating a possibly cooperative role of the bound and free PEI chains in gene delivery.

Fig. 6 also reveals that in the delayed addition of free PEI chains, i.e., t > 0, the gene transfection efficiency gradually decreases with the time interval between the administration of polyplexes and the addition of free PEI chains. To explain such a decrease, we have to find whether this decline is due to the insufficient incubation time since the incubation time was fixed to be 48 h, starting from the polyplex administration. The incubation-time dependence of the transgene expression, as shown in Fig. 7, clearly excludes such a possibility because the luciferase expression reaches its maximum at ~36 h after the polyplex administration. Therefore, the total 48-h incubation time is sufficient. The next question is whether these free PEI chains promote the cellular uptake in the extracellular space or other processes inside the cell. In the extracellular pathway, free PEI chains could facilitate the cellular internalization by increasing either the uptake rate or the endocytosis amount. To estimate the internalization time scale of the PEI/DNA dispersion, the cell culture medium with the polyplexes, if any, was replaced at different times after the polyplex administration.

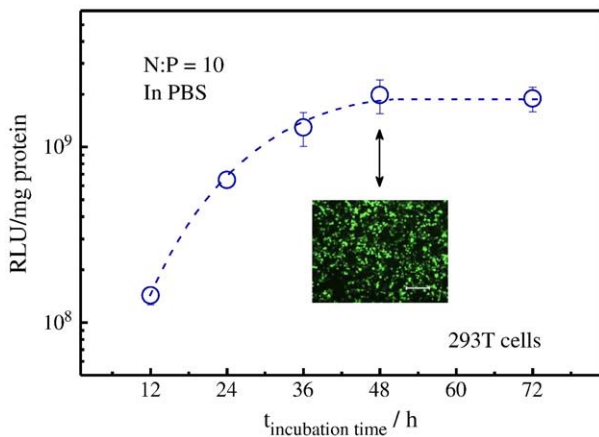


Fig. 7. Incubation-time dependence of luciferase expression of PEI/DNA polyplexes formed at N:P = 10. Inset: Fluorescent microscopic image of 293 T cells transfected with pEGFP-N1 after 48 h. Scale bar: 200 μm.

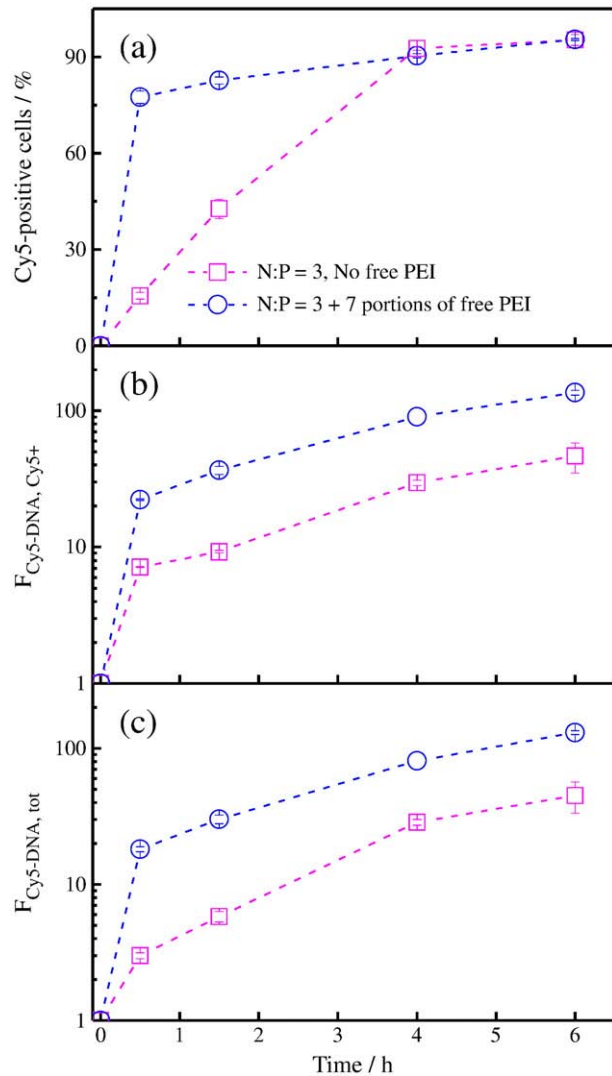


Fig. 9. Effect of free PEI chains on the internalization of PEI/DNA polyplexes by flow cytometry. 293 T cells were transfected with PEI/Cy5-DNA polyplexes alone (N:P = 3), or polyplexes plus 7 portions of free FITC-PEI (N:P = 10), harvested, and analyzed at the indicated time points. Internalization extent is expressed as (a) percentage of Cy5-positive cells; (b) median of Cy5-DNA fluorescence intensity of Cy5-positive cell population (F<sub>Cy5-DNA, Cy5+</sub>); and (c) median of Cy5-DNA fluorescence intensity of total cell population (F<sub>Cy5-DNA, tot</sub>).

Fig. 8 shows that the cellular uptake nearly ceases after ~6 h regardless of whether there are free PEI chains, but these free polycations enhance the final transfection levels by ~500 times even though they do not shorten the time required for internalization.

Furthermore, flow cytometry was used to explore the internalization kinetics of PEI/DNA polyplexes and free PEI chains in the gene transfection. Generally, three characteristics can be extracted from the flow cytometry data; namely, (i) the fraction of cells containing Cy5 fluorescence (Fig. 9a); (ii) the median of Cy5-DNA fluorescence intensity of Cy5-positive cell population ( $F_{\text{Cy5-DNA, Cy5+}}$ , Fig. 9b); and (iii) the median of Cy5-DNA fluorescence intensity of total cell population ( $F_{\text{Cy5-DNA, tot}}$ , Fig. 9c). Fig. 9a shows that in the presence of 7 portions of free PEI chains, more than 80% of the cells have internalized polyplexes after a 30-min incubation, whereas the internalized polyplexes without free PEI chains are detected in only ~10% of the cells. At 4 h post-incubation, ~95% of the cells are Cy5-positive regardless of the addition of free PEI chains. In addition,  $F_{\text{Cy5-DNA, Cy5+}}$ , which is indicative of the average amount of polyplexes inside each Cy5-positive cell, is stably 3–6 times higher during the first 6-h incubation when the extra 7 portions of PEI chains are applied (Fig. 9b). In combination, the addition of free PEI leads to a significant faster and remarkably increased internalization (Fig. 9c). Moreover, different uptake kinetics is revealed for polyplexes in the absence/presence of the free PEI chains (Fig. 10). When the polyplexes are applied alone, the number of cells they entered and their content per cell elevate simultaneously in the first 6 h of incubation. With the aid of 7 portions of free PEI chains, in contrast, the fraction of Cy5-positive cells quickly rises to ~80% within just 30 min, and the enhanced internalization afterwards (1.5–6 h) is mainly attributed to the increasing amount of polyplexes inside one cell.

On the other hand, the 7 portions of free PEI chains, whether applied alone or with PEI/DNA polyplexes at N:P=3, exhibit similar internalization kinetics (Fig. 11). Within just 30 min, these free PEI chains enter ~80% of the cells, with their intracellular fluorescence intensity almost reaching the maximum plateau. Moreover, our CLSM result also confirms that the concentrations of free PEI chains at the cellular membrane and inside the cell quickly approach to the maximum ~30 min after they are added outside the cell (Fig. 12). This indicates that the free PEI chains have a significantly faster uptake rate, and perhaps a different internalization pathway, compared to the PEI/DNA polyplexes (~6 h). Notably, the major uptake time scale of free PEI (~0.5–1.5 h) is in good accordance with the sharp increase in the

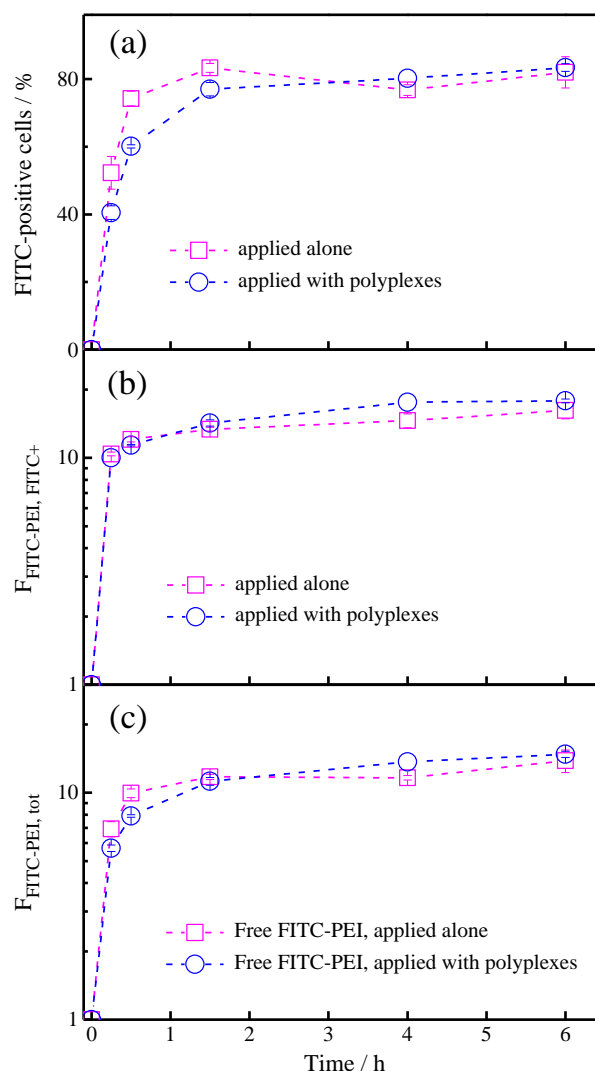


Fig. 11. Comparison of the internalization kinetics of free FITC-PEI chains applied alone or with PEI/DNA polyplexes of N:P = 3 in the gene transfection. Internalization extent is expressed as (a) percentage of FITC-positive cells; (b) median of FITC-PEI fluorescence intensity of FITC-positive cell population ( $F_{\text{FITC-PEI, FITC+}}$ ); and (c) median of FITC-PEI fluorescence intensity of total cell population ( $F_{\text{FITC-PEI, tot}}$ ).

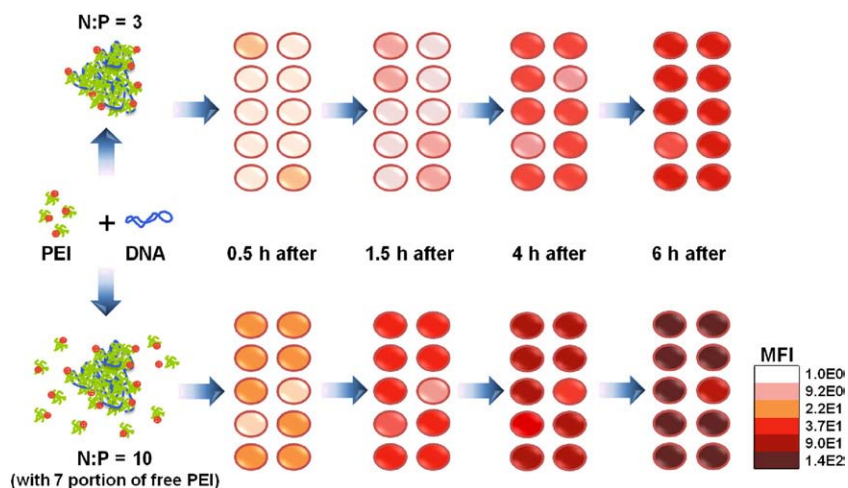
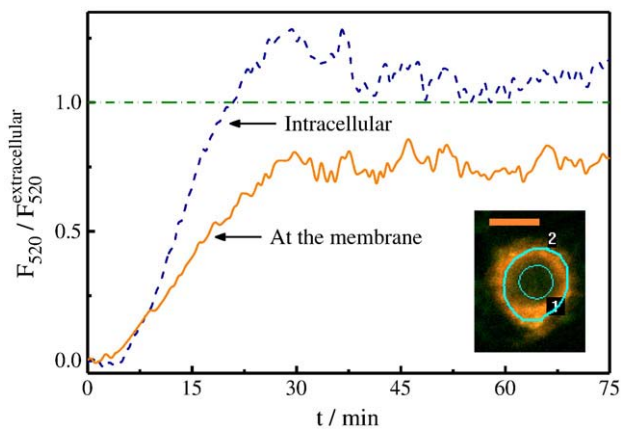


Fig. 10. Schematic illustration of cellular internalization of PEI/DNA polyplexes (N:P=3) in the absence and presence of 7 portions of free PEI chains, where different colors represents the median of DNA fluorescence intensity (MFI) inside one cell. Note that the depictions of different components do not reflect their actual sizes.



**Fig. 12.** Cellular membrane translocation kinetics of FITC-labeled bPEI-25 K chains, where the mean FITC-PEI fluorescence intensities at the membrane (on the circle 2) and inside the cell (inside circle 1, scale bar: 10  $\mu$ m) are normalized by that outside the cell.

number of polyplex-containing cells at N:P = 10 (Fig. 9a), suggesting that these excessive PEI chains might mainly play their roles in the first 1.5 h. It is still to be elucidated that how the free PEI chains promote the cellular internalization. They might either destabilize the cellular membrane to make the endocytosis of polyplexes more easily, or help the polyplexes to utilize an internalization pathway more favorable for intracellular trafficking [25,26,54].

To compare the contribution of free PEI chains in the extracellular and intracellular pathways, we added free PEI chains with or without removing the cell culture medium that contains the polyplexes (Fig. 13). Since the cellular internalization stops after  $\sim$ 6 h, those polyplexes in the extracellular space, if any, should still remain there. For N:P = 10, when the polyplexes are removed, at 6 h post-incubation, before the addition of 7 portions of free PEI chains, the gene transfection efficiency is only attenuated by 2-fold in comparison with the non-removal group, indicating that those free PEI chains promote the cellular uptake a little. However, it is worth noting that this reduced transfection efficiency is still  $\sim$ 50-fold higher than that without the addition of free PEI chains (N:P = 3), clearly indicating that the free PEI chains mainly play their role inside the cells.

Finally, we explored the effect of fetal bovine serum (FBS) on the gene transfection efficiency of polyplexes alone (N:P = 3), or polyplexes with 7 portions of free PEI chains added at different times (N:P = 10). When the cell culture medium is supplemented with 10% FBS, the initial transfection efficiency of polyplexes at N:P = 3 is reduced

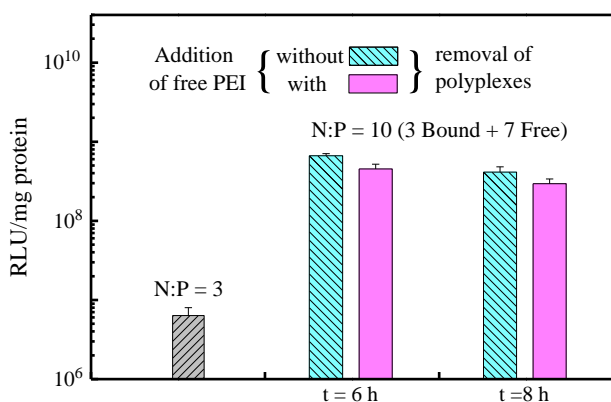


**Fig. 13.** Effect of free PEI chains on the intracellular trafficking of PEI/DNA polyplexes formed in PBS, where 7 portions of free PEI chains were added, respectively, at 6 h and 8 h post-administration of the polyplexes (N:P = 3), with or without the removal of cell culture medium.

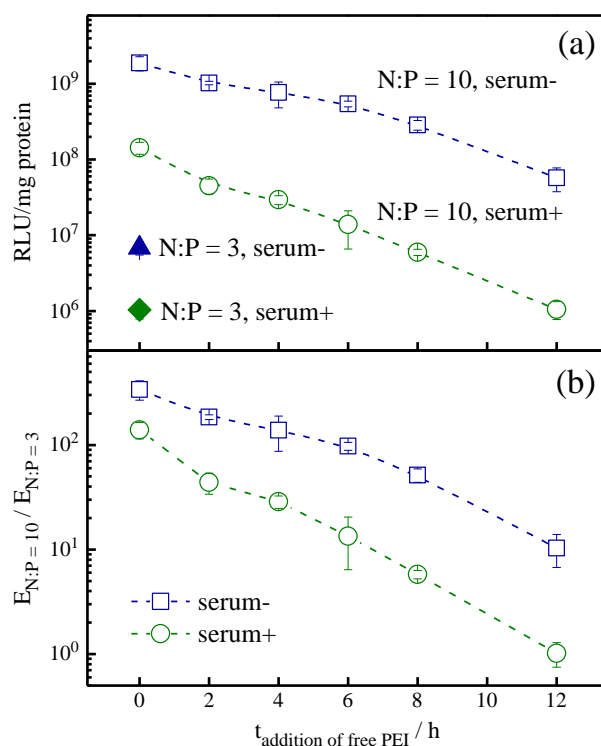


**Fig. 14.** (a) Effect of FBS (10% in the cell culture medium) on the transfection efficiency of polyplexes alone (N:P = 3), or polyplexes with 7 portions of free PEI added at different times (N:P = 10). (b) Relative transfection efficiency of polyplexes plus free PEI ( $E_{N:P=10}$ ) to polyplex alone ( $E_{N:P=3}$ ) in the serum-free (-) and serum-containing (+) medium, respectively. The cell culture medium is not replaced before the addition of free PEI chains.

by  $\sim$ 5 times (Fig. 14a). Moreover, the 7 portions of free PEI chains added afterwards only increase the transfection level by 1–150 folds, whereas, in the serum-free medium, they can enhance the transfection efficiency by 10–300 times (Fig. 14b). This decreased efficacy is mainly attributed to the association of the cationic polyplexes and PEI chains with the negatively charged proteins in FBS; namely, it reduces the effective amount of free PEI chains, which indirectly supports our finding that free PEI chains plays a significant role in promoting the transfection. Therefore, for the future *in vivo* study, we have to consider how to incorporate free PEI chains together with polyplexes and keep their integrity in the blood stream so that they can be safely delivered to the targeted cells or organs.

In sum, our results reveal the existence of some cooperative actions between the polyplexes and free polycationic chains. The cationic PEI chains inside each polyplex condense anionic DNA chains into a small and compact particle so that the endocytosis is facilitated. These bound PEI chains also shield DNA from the intracellular degradation; while those free PEI chains in the solution mixture mainly navigate some unknown intracellular trafficking barriers, including endolysosomal formation and/or escape and the subsequent nuclear localization. It is a remaining challenge to map these intracellular trafficking pathways and understand how free PEI chains exactly promote the gene transfection inside the cell by using various existing tools of molecular biology.

#### 4. Conclusion

A combination of laser light scattering (LLS) and gel electrophoresis results confirms that most of anionic DNA chains are complexed and condensed by cationic PEI chains when the molar ratio of nitrogen from PEI to phosphate from DNA (N:P) reaches  $\sim$ 3, independent of the PEI chain length and solvent (pure water or PBS), revealing that the



charge neutrality (electrostatic interaction) is the main driving force for the polyplex formation. In the solution mixture with  $N:P > 3$ , there are two kinds of PEI chains: bound to DNA and free in the solution mixture. The bound PEI chains inside the polyplexes provide a charge compensation so that DNA is condensed and protected from degradation. Our current study convincingly reveals that it is those free PEI chains, rather than other physical properties of the PEI/DNA polyplexes, that play a vital role in promoting the gene transfection. The addition of free PEI leads to a significant faster and more efficient cellular uptake of polyplexes, but these free PEI chains mainly contribute to the subsequent intracellular trafficking. Our finding leads to a different thinking in the development of non-viral vectors; namely, we might not need to invest much of our effort on the synthesis of different cationic polymers, but focus on how the free polycationic chains promote the intracellular trafficking of the polyplexes. As for *in vivo* experiments, we have to consider how to incorporate free chains together with polyplexes and keep their integrity during circulation so that they can be safely delivered to the targeted cells or organs.

### Acknowledgements

The financial support of the National Natural Scientific Foundation of China (NNSFC) Projects (50773077 and 20934005) and the Hong Kong Special Administration Region Earmarked (RGC) Projects (CUHK4037/07P, 2160331; CUHK4046/08P, 2160365; CUHK4039/08P, 2160361; and CUHK4042/09P, 2160396) is gratefully acknowledged.

### Appendix A. Supplementary data

Supplementary data to this article can be found online at doi:10.1016/j.jconrel.2010.10.028.

### References

- [1] E. Check, Gene therapy: a tragic setback, *Nature* 420 (6912) (2002) 116–118.
- [2] S.E. Raper, N. Chirmule, F.S. Lee, N.A. Wivel, A. Bagg, G.P. Gao, J.M. Wilson, M.L. Batshaw, Fatal systemic inflammatory response syndrome in an ornithine transcarbamylase deficient patient following adenoviral gene transfer, *Mol. Genet. Metab.* 80 (1–2) (2003) 148–158.
- [3] S. Hacia-Bey-Abina, LMO2-associated clonal T cell proliferation in two patients after gene therapy for SCID-X1, *Science* 302 (5644) (2003) 415–419.
- [4] D.W. Pack, A.S. Hoffman, S. Pun, P.S. Stayton, Design and development of polymers for gene delivery, *Nat. Rev. Drug Discov.* 4 (7) (2005) 581–593.
- [5] S.D. Li, L. Huang, Non-viral is superior to viral gene delivery, *J. Control. Release.* 123 (3) (2007) 181–183.
- [6] M.A. Mintzer, E.E. Simanek, Nonviral vectors for gene delivery, *Chem. Rev.* 109 (2) (2009) 259–302.
- [7] O. Boussif, F. Lezoualch, M.A. Zanta, M.D. Mergny, D. Scherman, B. Demeneix, J.P. Behr, A versatile vector for gene and oligonucleotide transfer into cells in culture and *in vivo* – polyethylenimine, *Proc. Natl. Acad. Sci. U. S. A.* 92 (16) (1995) 7297–7301.
- [8] U. Lungwitz, M. Breunig, T. Blunk, A. Gopferich, Polyethylenimine-based non-viral gene delivery systems, *Eur. J. Pharm. Biopharm.* 60 (2) (2005) 247–266.
- [9] M. Neu, D. Fischer, T. Kissel, Recent advances in rational gene transfer vector design based on poly(ethylene imine) and its derivatives, *J. Gene Med.* 7 (8) (2005) 992–1009.
- [10] M. Breunig, U. Lungwitz, R. Liebl, A. Gopferich, Breaking up the correlation between efficacy and toxicity for nonviral gene delivery, *Proc. Natl. Acad. Sci. U. S. A.* 104 (36) (2007) 14454–14459.
- [11] R. Deng, Y. Yue, F. Jin, Y. Chen, H. Kung, M. Lin, C. Wu, Revisit the complexation of PEI and DNA – How to make low cytotoxic and highly efficient PEI gene transfection non-viral vectors with a controllable chain length and structure? *J. Control. Release.* 140 (1) (2009) 40–46.
- [12] M. Ogris, S. Brunner, S. Schuller, R. Kircheis, E. Wagner, PEGylated DNA/transferrin-PEI complexes: reduced interaction with blood components, extended circulation in blood and potential for systemic gene delivery, *Gene Ther.* 6 (4) (1999) 595–605.
- [13] H. Cheng, J.L. Zhu, X. Zeng, Y. Jing, X.Z. Zhang, R.X. Zhuo, Targeted gene delivery mediated by folate-polyethylenimine-block-poly(ethylene glycol) with receptor selectivity, *Bioconjugate Chem.* 20 (3) (2009) 481–487.
- [14] M.A. Zanta, O. Boussif, A. Adib, J.P. Behr, *In vitro* gene delivery to hepatocytes with galactosylated polyethylenimine, *Bioconjugate Chem.* 8 (6) (1997) 839–844.
- [15] S.S. Diebold, P. Kursa, E. Wagner, M. Cotten, M. Zenke, Mannose polyethylenimine conjugates for targeted DNA delivery into dendritic cells, *J. Biol. Chem.* 274 (27) (1999) 19087–19094.
- [16] H. Pollard, J.S. Remy, G. Loussouarn, S. Demolombe, J.P. Behr, D. Escande, Polyethylenimine but not cationic lipids promotes transgene delivery to the nucleus in mammalian cells, *J. Biol. Chem.* 273 (13) (1998) 7507–7511.
- [17] W.T. Godbey, K.K. Wu, A.G. Mikos, Tracking the intracellular path of poly(ethylenimine)/DNA complexes for gene delivery, *Proc. Natl. Acad. Sci. U. S. A.* 96 (9) (1999) 5177–5181.
- [18] T. Bieber, W. Meissner, S. Kostin, A. Niemann, H.P. Elsasser, Intracellular route and transcriptional competence of polyethylenimine-DNA complexes, *J. Control. Release.* 82 (2–3) (2002) 441–454.
- [19] N.D. Sonawane, F.C. Szoka, A.S. Verkman, Chloride accumulation and swelling in endosomes enhances DNA transfer by polyamine-DNA polyplexes, *J. Biol. Chem.* 278 (45) (2003) 44826–44831.
- [20] J. Suh, D. Wirtz, J. Hanes, Efficient active transport of gene nanocarriers to the cell nucleus, *Proc. Natl. Acad. Sci. U. S. A.* 100 (7) (2003) 3878–3882.
- [21] A. Akinc, M. Thomas, A.M. Klibanov, R. Langer, Exploring polyethylenimine-mediated DNA transfection and the proton sponge hypothesis, *J. Gene Med.* 7 (5) (2005) 657–663.
- [22] R.P. Kulkarni, D.D. Wu, M.E. Davis, S.E. Fraser, Quantitating intracellular transport of polyplexes by spatio-temporal image correlation spectroscopy, *Proc. Natl. Acad. Sci. U. S. A.* 102 (21) (2005) 7523–7528.
- [23] K. de Bruin, N. Ruthardt, K. von Gersdorff, R. Bausinger, E. Wagner, M. Ogris, C. Brauchle, Cellular dynamics of EGF receptor-targeted synthetic viruses, *Mol. Ther.* 15 (7) (2007) 1297–1305.
- [24] K.G. de Bruin, C. Fella, M. Ogris, E. Wagner, N. Ruthardt, C. Brauchle, Dynamics of photoinduced endosomal release of polyplexes, *J. Control. Release.* 130 (2) (2008) 175–182.
- [25] N.P. Gabrielson, D.W. Pack, Efficient polyethylenimine-mediated gene delivery proceeds via a caveolar pathway in HeLa cells, *J. Control. Release.* 136 (1) (2009) 54–61.
- [26] Y.Y. Won, R. Sharma, S.F. Konieczny, Missing pieces in understanding the intracellular trafficking of polycation/DNA complexes, *J. Control. Release.* 139 (2) (2009) 88–93.
- [27] H. Lee, I.K. Kim, T.G. Park, Intracellular trafficking and unpacking of siRNA/quantum dot-PEI complexes modified with and without cell penetrating peptide: confocal and flow cytometric FRET analysis, *Bioconjugate Chem.* 21 (2) (2010) 289–295.
- [28] E. Wagner, M. Cotten, R. Foisner, M.L. Birnstiel, Transferrin polycation DNA complexes – the effect of polycations on the structure of the complex and DNA delivery to cells, *Proc. Natl. Acad. Sci. U. S. A.* 88 (10) (1991) 4255–4259.
- [29] W.T. Godbey, K.K. Wu, A.G. Mikos, Size matters: molecular weight affects the efficiency of poly(ethylenimine) as a gene delivery vehicle, *J. Biomed. Mater. Res.* 45 (3) (1999) 268–275.
- [30] L. Wightman, R. Kircheis, V. Rossler, S. Carotta, R. Ruzicka, M. Kursa, E. Wagner, Different behavior of branched and linear polyethylenimine for gene delivery *in vitro* and *in vivo*, *J. Gene Med.* 3 (4) (2001) 362–372.
- [31] K. Kunath, A. von Harpe, D. Fischer, B. Peterson, U. Bickel, K. Voigt, T. Kissel, Low-molecular-weight polyethylenimine as a non-viral vector for DNA delivery: comparison of physicochemical properties, transfection efficiency and *in vivo* distribution with high-molecular-weight polyethylenimine, *J. Control. Release.* 89 (1) (2003) 113–125.
- [32] I. Honore, S. Grosse, N. Frison, F. Favatier, M. Monsigny, I. Fajac, Transcription of plasmid DNA: influence of plasmid DNA/polyethylenimine complex formation, *J. Control. Release.* 107 (3) (2005) 537–546.
- [33] S.H. Pun, N.C. Bellocq, A.J. Liu, G. Jensen, T. Machemer, E. Quijano, T. Schluep, S.F. Wen, H. Engler, J. Heidel, M.E. Davis, Cyclodextrin-modified polyethylenimine polymers for gene delivery, *Bioconjugate Chem.* 15 (4) (2004) 831–840.
- [34] T. Ooya, H.S. Choi, A. Yamashita, N. Yui, Y. Sugaya, A. Kano, A. Maruyama, H. Akita, R. Ito, K. Kogure, H. Harashima, Biodegradable polyrotaxane – Plasmid DNA polyplex for enhanced gene delivery, *J. Am. Chem. Soc.* 128 (12) (2006) 3852–3853.
- [35] H.Y. Tian, W. Xiong, J.Z. Wei, Y. Wang, X.S. Chen, X.B. Jing, Q.Y. Zhu, Gene transfection of hyperbranched PEI grafted by hydrophobic amino acid segment PBLG, *Biomaterials* 28 (18) (2007) 2899–2907.
- [36] Y.X. Sun, W. Xiao, S.X. Cheng, X.Z. Zhang, R.X. Zhuo, Synthesis of (Dex-HMDI)-g-PEIs as effective and low cytotoxic nonviral gene vectors, *J. Control. Release.* 128 (2) (2008) 171–178.
- [37] B. Liang, M.L. He, C.Y. Chan, Y.C. Chen, X.P. Li, Y. Li, D.X. Zheng, M.C. Lin, H.F. Kung, X.T. Shuai, Y. Peng, The use of folate-PEG-grafted-hyperbranched-PEI nonviral vector for the inhibition of glioma growth in the rat, *Biomaterials* 30 (23–24) (2009) 4014–4020.
- [38] BloomfieldV.A., DNA condensation by multivalent cations, *Biopolymers* 44 (3) (1997) 269–282.
- [39] E. Lai, J.H. van Zanten, Monitoring DNA/poly-L-lysine polyplex formation with time-resolved multiangle laser light scattering, *Biophys. J.* 80 (2) (2001) 864–873.
- [40] E. Vuorimaa, A. Urtti, R. Seppanen, H. Lemmetyinen, M. Yliperttula, Time-resolved fluorescence spectroscopy reveals functional differences of cationic polymer-DNA complexes, *J. Am. Chem. Soc.* 130 (35) (2008) 11695–11700.
- [41] J. Ziebarth, Y.M. Wang, Molecular dynamics simulations of DNA-polycation complex formation, *Biophys. J.* 97 (7) (2009) 1971–1983.
- [42] J.P. Behr, The proton sponge: a trick to enter cells the viruses did not exploit, *Chimia* 51 (1–2) (1997) 34–36.
- [43] J.P. Clamme, J. Azoulay, Y. Mely, Monitoring of the formation and dissociation of polyethylenimine/DNA complexes by two photon fluorescence correlation spectroscopy, *Biophys. J.* 84 (3) (2003) 1960–1968.
- [44] S. Boeckle, K. von Gersdorff, S. van der Piepen, C. Culmsee, E. Wagner, M. Ogris, Purification of polyethylenimine polyplexes highlights the role of free polycations in gene transfer, *J. Gene Med.* 6 (10) (2004) 1102–1111.

- [45] J. Fahrmeir, M. Gunther, N. Tietze, E. Wagner, M. Ogris, Electrophoretic purification of tumor-targeted polyethylenimine-based polyplexes reduces toxic side effects in vivo, *J. Control. Release*. 122 (3) (2007) 236–245.
- [46] J.P. Clamme, G. Krishnamoorthy, Y. Mely, Intracellular dynamics of the gene delivery vehicle polyethylenimine during transfection: investigation by two-photon fluorescence correlation spectroscopy, *Biochim. Biophys. Acta, Biomembr.* 1617 (1–2) (2003) 52–61.
- [47] J.M. Saul, C.H.K. Wang, C.P. Ng, S.H. Pun, Multilayer nanocomplexes of polymer and DNA exhibit enhanced gene delivery, *Adv. Mater.* 20 (6) (2008) 19–25.
- [48] B. Berne, R. Pecora, *Dynamic Light Scattering*, Plenum Press, New York, 1976.
- [49] B. Chu, *Laser Light Scattering*, second ed. Academic Press, New York, 1991.
- [50] R.J. Hunter, *Foundations of Colloid Science*, second ed. Oxford Press, Oxford, 2000.
- [51] M.L. Forrest, D.W. Pack, On the kinetics of polyplex endocytic trafficking: implications for gene delivery vector design, *Mol. Ther.* 6 (1) (2002) 57–66.
- [52] M. Breunig, U. Lungwitz, R. Liebl, C. Fontanari, J. Klar, A. Kurtz, T. Blunk, A. Goeferich, Gene delivery with low molecular weight linear polyethylenimines, *J. Gene Med.* 7 (10) (2005) 1287–1298.
- [53] C. Wu, K.Q. Xia, Incorporation of a differential refractometer into a laser light-scattering spectrometer, *Rev. Sci. Instrum.* 65 (3) (1994) 587–590.
- [54] J. Rejman, A. Bragonzi, M. Conese, Role of clathrin- and caveolae-mediated endocytosis in gene transfer mediated by lipo- and polyplexes, *Mol. Ther.* 12 (3) (2005) 468–474.